HHS Public Access

Author manuscript

ACS Chem Biol. Author manuscript; available in PMC 2018 June 16.

Published in final edited form as:

ACS Chem Biol. 2017 June 16; 12(6): 1691–1702. doi:10.1021/acschembio.7b00241.

Citrullination/methylation crosstalk on histone H3 regulates ER-target gene transcription

Kathleen W. Clancy[1,2], **Anna-Maria Russell**[1], **Venkataraman Subramanian**[2], **Hannah Nguyen**[1], **Yuewei Qian**[1], **Robert M. Campbell**[1], and **Paul R. Thompson**[2,3,*]

[1]Lilly Research Laboratories, Eli Lilly & Company, Indianapolis, IN, 46285

[2]Department of Biochemistry and Pharmacology, University of Massachusetts Medical School, Worcester, MA, 01605

[3]Program in Chemical Biology, UMass Medical School, 364 Plantation Street, Worcester, MA 01605, USA

Abstract

Posttranslational modifications of histone tails are a key contributor to epigenetic regulation. Histone H3 Arg26 and Lys27 are both modified by multiple enzymes and their modifications have profound effects on gene expression. Citrullination of H3R26 by PAD2 and methylation of H3K27 by PRC2 have opposing downstream impacts on gene regulation; H3R26 citrullination activates gene expression and H3K27 methylation represses gene expression. Both of these modifications are drivers of a variety of cancers and their writer enzymes, PAD2 and EZH2, are the target of drug therapies. After biochemical and cell-based analysis of these modifications, a negative crosstalk interaction is observed. Methylation of H3K27 slows citrullination of H3R26 30-fold, whereas citrullination of H3R26 slows methylation 30,000-fold. Examination of the mechanism of this crosstalk interaction uncovered a change in structure of the histone tail upon citrullination which prevents methylation by the PRC2 complex. This mechanism of crosstalk is reiterated in cell lines using knockdowns and inhibitors of both enzymes. Based our data, we propose a model in which, after H3Cit26 formation, H3K27 demethylases are recruited to the chromatin to activate transcription. In total, our studies support the existence of crosstalk between citrullination of H3R26 and methylation of H3K27.

Introduction

Posttranslational modifications (PTMs) of the histone tails of chromatin have long been understood to be one of the key regulatory mechanisms that control eukaryotic gene

*Author to whom correspondence should be addressed: Paul R. Thompson paul.thompson@umassmed.edu, Tel: 508-856-8492.

ORCID

Paul R. Thompson: 0000-0002-1621-3372

Notes

The authors declare the following competing financial interest(s): P.R.T. is a consultant to Bristol-Myers Squibb. The remaining authors have no competing interest to declare.

Supporting Information

Figures S1–S3, and Tables S1–S4. This material is available free of charge on the ACS Publications websites at DOI:

expression.[1–3] The epigenetic landscape, however, has been further complicated by a plethora of other processes including chromatin remodeling,[3–5] DNA methylation,[6] and PTM crosstalk.[7–9] PTM crosstalk is a documented source of complexity serving as a regulatory mechanism on both histone and non-histone proteins.[10, 11]

Protein citrullination (deimination) is a PTM catalyzed by the Protein Arginine Deiminase (PAD) family of enzymes. Compared to more canonical PTMs like methylation and acetylation, citrullination is relatively uncharacterized.[12, 13] Citrullination is the transformation of the terminal guanidinium group of an arginine to a urea, neutralizing the positive charge of this residue. While the change in molecular weight is minimal (+0.98 Da), neutralizing the positive charge is significant and can affect protein structure and catalysis as well as protein-protein and protein-nucleic acid interactions. Histone citrullination occurs on Histone H1,[14] H2A,[15] H3,[16, 17] and H4[18] and can have either activating or silencing effects on transcription.[17–19] While most studies of citrullination and PAD activity focus on autoimmune and inflammatory disease,[19–21] applications in cancer have also been explored.[22, 23] Specifically, in breast cancer, PAD inhibition has been shown to be a potential route of therapy.[17, 24–26] Notably, PAD2 is highly expressed in breast cancer and contributes to cell proliferation via its ability to citrullinate H3R26, which drives the expression of ERα-target genes in ER-positive breast cancer.[27] Citrullination of H3R26 was shown to occur on the promoters of a number of ER-responsive genes in MCF7 cells. This PTM was reduced in PAD2 knockdown cells, along with transcript levels of target genes, establishing a mechanistic relevance for PAD2 in ER (+) breast cancer.[17]

The neighboring residue, on histone H3, Lys27 (H3K27), is methylated by EZH2. Di- and Tri-methylated H3K27 is a repressive pro-oncogenic mark described in numerous cancers including leukemia,[17] lymphoma,[28, 29] bladder,[30] colon,[31] glioma,[32] and ovarian.[33] In addition to the oncogenic effect of EZH2, activating mutations of the enzyme have been shown to generate higher levels of trimethylated H3K27 ($H3K27Me_3$).[29, 34] Cancers with these mutations are associated with poor prognosis.[35]

Inhibition of EZH2 is of great interest as a potential treatment for these conditions and a number of compounds have emerged as potential therapeutics.[29, 30, 36, 37] EZH2 is a component of the polycomb repressive complex 2 (PRC2) along with Suz12, EED, and other accessory proteins. While Suz12 and EED are required for the methyltransferase activity of PRC2, the other members of the complex are not.[38, 39] Disruption of the PRC2 complex is also an effective method of inactivating EZH2 function.[40] Notably, methylation and other modifications on H3K27 are highly dynamic. Demethylases (UTX, JMJD3), acetyltransferases (p300/CBP) and deacetylases (HDAC1/2) all impact the posttranslational modifications present on H3K27.[41]

Given the significance of both the H3Cit26 and $H3K27Me_3$ marks, information concerning the crosstalk between these two PTMs is critical in designing epigenetic therapeutic strategies. Herein, we show that citrullination of H3R26 inhibits methylation of H3K27 by both wild-type (wt) and mutant EZH2. We also show that methylation of H3K27 impairs the citrullination of H3R26 by PAD2. This example of negative crosstalk is recapitulated in cells where we show that in B cell lymphoma lines, knockdown or inhibition of one enzyme

results in an increased level of the alternate PTM. In ER (+) breast cancer cell lines, an inducible system of H3Cit26 formation, a more complex mechanism of crosstalk is observed involving the recruitment of the histone lysine demethylases UTX and JMJD3 and the regulation of the GDNF-RET pathway, which is implicated in aromatase inhibitor resistance.

Results and Discussion

Citrullination of Histone H3 Blocks its Methylation by the PRC2 Complex

To initially evaluate the potential for crosstalk between the citrullination of H3R26 and methylation of H3K27, we first incubated recombinant H3 with either PAD2 or PAD4 for 60 min to allow for complete citrullination. *In vitro*, both isozymes have been shown to citrullinate histone H3 on R2, R8, R17 and R26.[18, 42] Following this incubation, PRC2, along with its cofactor, S-adenosyl methionine (SAM) was added to prompt methylation of H3K27. Compared to the buffer control, PAD2 and PAD4 preincubation both reduced the PRC2-catalyzed methylation activity by more than 75% (Figure 1B). The effect of PAD2 was particularly robust, blocking more than 90% of PRC2 activity. This loss in activity is dependent upon citrullination as both PAD2 and PAD4 were able to decrease PRC2 catalyzed methylation in a time- and dose-dependent manner (Figure S1A and B). Formation of H3Cit26 and H3K27Me_3 was confirmed by Western blotting (Figure S1C).

Methylation of Histone H3 by the PRC2 Complex Blocks PAD Activity

In the reverse experiment, Histone H3 was incubated with PRC2 and SAM for 120 min to allow for methylation of H3K27, the only site of methylation catalyzed by PRC2 on Histone H3.[17] Following the methylation reaction, PAD2 or PAD4 was added to the mixture and allowed to citrullinate the histone for 30 min. Total citrulline levels were determined using a citrulline-specific chemical probe, Rh-PG.[43] As in the previous experiments, methylation of H3K27 negatively impacted the ability of PAD2 and PAD4 to citrullinate histone H3 (Figure 1C). Together, these two experiments establish the biochemical potential for negative crosstalk between the PADs and PRC2 on Histone H3 (Figure 1A).

Citrullination of PRC2 does not affect its methyltransferase activity

To rule out the possibility that the observed decrease in methylation of Histone H3 is due to the citrullination of PRC2, we conducted two experiments using the pan-PAD inhibitor F-Amidine.[44, 45] First, Histone H3 was incubated with either PAD2 or PAD4 for 60 min. Both samples were then treated with F-Amidine to irreversibly inhibit PAD activity before adding PRC2 and SAM to assay residual methyltransferase activity; F-Amidine is a highly selective, irreversible pan-PAD inhibitor.[46] As shown in Figure 2A, incubation of Histone H3 with PAD2 greatly decreased the methyltransferase activity of PRC2. These data are consistent with the notion that the decrease in PRC2 activity is due to the citrullination of Histone H3. Second, PRC2 was incubated with the PAD isozymes followed by the inhibition of PAD activity with F-Amidine. Histone H3 and SAM were then added to evaluate the effect on the methyltransferase activity of PRC2. As depicted in Figure 2B, the methyltransferase activity of PRC2 was not affected by this treatment. In total, these data indicate that the inhibitory effect of PAD incubation on PRC2 activity is due to the modification of Histone H3 rather than a direct modification of PRC2.

Citrullination of H3R26 blocks PRC2-catalyzed methylation of H3K27

As PAD2 and PAD4 citrullinate multiple sites on Histone H3 *in vitro,*[18, 46] we synthesized a series of Histone H3 peptide tail analogs, centered around H3K27, that only contain one arginine, H3R26. These peptides, which are comprised of residues from 23–39, were used to evaluate the effects of citrullination at H3R26 on PRC2 activity. Initially, AcH3[23–39] was incubated with PAD2 before treatment with PRC2 and SAM. Consistent with our previous findings with Histone H3, methylation of the peptide was greatly reduced (Figure 2C). In contrast, preincubation with PAD4 showed little effect on methylation. The latter result is explained by the fact that PAD2 (and not PAD4) preferentially modifies H3R26 *in vitro* and *in vivo.*[17]

To more directly evaluate crosstalk between these two modifications, we incorporated citrulline in the place of R26 in the AcH3[23–39] peptide. Notably, we were unable to detect any methyl transfer to the citrulline containing peptide or to the negative control K27Ac peptide (Figure 2D). These studies confirm that the presence of an arginine at position 26 of histone H3 is critical for proper substrate recognition by PRC2.

To further explore this phenomenon, the steady-state kinetic parameters for PRC2 complexes containing either WT (Figure 2E, Table S2) or mutant (Figure 2F, Table S3) EZH2 (Y641N) were determined with a variety of histone H3 substrates. As described in previous publications,[17] the monomethylated peptide is the best substrate for wt EZH2. Other reports postulate that EZH1 is primarily responsible for monomethylating H3K27 whereas EZH2 performs the di- and tri-methylation processes.[47, 48] That data is upheld in this study with an increase in catalytic efficiency of over 100-fold when comparing the monomethylated peptide to the unmodified peptide. Compared to the unmodified peptide, the k_{cat}/K_M for the Cit26 peptide is decreased more than 1,000-fold. Cit26 was also incorporated into a peptide with different methylation states of K27 in order to probe the most efficient potential substrates for EZH2. Consistent with the above results, the replacement of R26 with citrulline in the AcH3[23–39] K27Me$_1$ peptide, causes k_{cat}/K_M to decrease by a factor of over 10^4-fold. These results reveal a crucial role for H3R26 in substrate recognition.

Activating mutations of EZH2 in PRC2 have been described in B-cell lymphoma.[35, 47] These mutations cause hyper-trimethylation of H3K27, exacerbating the repressive traits of this PTM and increasing the oncogenic nature of the tumor.[36, 49, 50] The hypothesis for the increased trimethylation activity is a more open active site cavity, allowing for the binding of a bulkier, dimethylated lysine substrate.[51, 52] The question then arose if citrullination at H3R26 would also impede K27 methylation in the activating mutation of EZH2, Y641N. The same substrates tested against wt EZH2 were also tested with EZH2 Y641N (Figure 2F, Table S3). As expected, the best substrate for the activated EZH2 mutant was the dimethylated K27 peptide ($k_{cat}/K_M = 1.2 \times 10^3$ $M^{-1}min^{-1}$). Any peptide containing citrulline in the 26 position showed a >1,000-fold decrease in activity. For example, comparing AcH3[23–39] K27Me$_2$ and AcH321–39 Cit26K27Me$_2$ peptides, the catalytic efficiency is decreased by 10,000-fold. Thus, the EZH2 (Y641N) mutant does not overcome the barrier of citrullination and further confirms the essential role of H3R26 in substrate recognition.

Increasing methylation states of K27 reduce citrullination of R26

The peptide-based Histone H3 substrates described above were also pretreated with PRC2 complex and PAD activity on these substrates was evaluated. The results show that methylation decreases citrullination catalyzed by either PAD2 or PAD4 (Figure 3A). Analogs were also synthesized with increasing methylation states at K27 to include mono-, di-, and trimethylated lysine. As shown in Figure 3B, monomethylation of K27 has little effect on PAD2 activity. However, di- and tri-methylation significantly inhibits citrullination of H3R26. Trimethylation of K27 results in a ~30-fold drop in catalytic efficiency. The kinetic analysis of PAD2 activity on these peptide substrates is summarized in Figure 3C and Table S3.

Structural Rationale for PTM Crosstalk

In an effort to provide an explanation for the observed negative crosstalk interaction, peptides derived from the histone H3 sequence were examined in the PRC2 complex (PDB ID: 5HYN) and in PAD4 (PDB ID: 3B1U) with the PAD2 structure (PDB ID: 4N2C) overlaid. The PRC2 structure contains H3 peptide H3[21–33] with the K27M mutation. After changing position 27 back to a lysine and minimizing energies in the binding site, we then calculated interaction energies between H3 wt and R26Cit peptides. The PAD4 structure used was solved with a substrate-based inhibitor (o-F-Amidine), allowing for facile modeling of H3 peptide substrates into the active site preserving R26 secondary structure according to the structure of o-F-Amidine in PAD4. PAD2 structures bound to substrate have not been determined. However, this isozyme shows strong structural and sequence homology with PAD4 (>75% of the catalytic domain).

Interaction energies for the enzyme/substrate interaction were calculated for both the native sequence and the sequence containing the crosstalk modification for both enzymes. Focusing first on PAD2, trimethylation of H3K27 decreases the binding interaction by ~31.5 kcal/mol (Figure 4A). This change is due to the loss of hydrogen bonding interactions between the K27 sidechain and carboxylate residues on PAD2 as well as weaker Van der Walls interactions. There are no observable steric clashes between the methyl groups on K27 and PAD2. For PRC2, the change in binding energy upon citrullination of R26 is only 15 kcal/mol. This small change is consistent with a lack of major structural perturbations and only minor alterations in the distances between R26 and the enzyme (Figure 4B). Despite considering possible electrostatic and non-bonded effects of substrate/enzyme interactions, these calculations fail to account for the $>10^3$-fold change in activity observed upon citrullination. Therefore, we further investigated the effect of PTMs on the substrate itself, electronically and structurally.

For these studies, each histone peptide (i.e., wt, R26Cit and K27Me3) was examined through 10 ns dynamics simulations to understand the peptides' conformational space preferences before and after modification. Crystal structures of PRC2 and PAD4 provide conformational preferences, measured by ΦΨ angles, for H3 to be a substrate for each of these enzymes. In PRC2, K27 adopts a β conformation while, in PAD4, R26 prefers an α conformation. With this knowledge we analyzed the dynamics trajectory by calculating ΦΨ angles for each annealed conformation. Analysis of the ΦΨ angles at position 26 and position 27 of these

peptides involved 1600 annealed conformers resulting from 10 ns simulations. Ramachandran plots summarizing these data are depicted in Figure 4C,D. The conformation of R26 (Figure 4C) undergoes only very minor changes upon trimethylation of K27, adopting a slight increase in α-turn character. In contrast, citrullination of the peptide, dramatically alters the positioning of K27 and the Ramachandran plot indicates a complete change from β-character to α-character (Figure 4D). Helping to validate our models, the peptide dynamics simulations generated conformations of wt H3 peptides similar to that found in the crystal structure of PRC2 (Figure S2). Moreover, an increase in α-helical character is also observed by CD analysis when comparing the R26Cit peptide with the wt sequence (Figure S3).

Taken together, the structure based modeling and dynamics simulations indicate that the capability of PAD2 to citrullinate substrates with trimethylated K27 is mainly reduced by less favorable enzyme/substrate interactions with minimal impact due to the conformation of the trimethylated peptide substrate. However, methylation of citrullinated substrates is only slightly affected by enzyme/substrate interactions. Instead, the dynamics simulation suggest that R26 citrullination causes a conformation that precludes its methylation by the PRC2 complex.

Cellular models of PTM crosstalk

To investigate this example of negative crosstalk in a cellular context, diffuse large B-cell lymphoma (DLBCL) lines (which express high levels of both PAD2 and EZH2) were manipulated by either knocking down or inhibiting PAD2 or EZH2 and evaluating the levels of different PTMs. Upon stable lentiviral knockdown of EZH2 in SU-DHL-10 cells, $H3K27Me_3$ levels drop and H3Cit26 levels increase dramatically, consistent with the negative crosstalk observed in biochemical assays (Figure 5A). Cells were then treated with EZH2 or PAD2 siRNA expressing lentivirus, treated with the EZH2 inhibitor EPZ-6438 or the PAD inhibitor BB-F-Amidine, or a combination of knockdown and inhibitor treatment. $H3K27Me_3$ levels show a 4-fold increase in the PAD2 knockdown cells and also in the cells treated with this PAD inhibitor. This effect is attenuated when the PAD2 knockdown cells are treated with the EZH2 inhibitor or the EZH2 knockdown cells are treated with PAD inhibitor, emphasizing the antagonistic relationship between these two PTMs (Figure 5B).

To further explore this relationship in cell systems with inducible citrullination, we examined two ER (+) breast cancer cell lines, MCF7 and T47D. These cells were stimulated with estradiol (E2) following hormone starvation for 48 h. In this inducible model of H3Cit26 formation,[53] both lines show an increase in H3Cit26 at 30–60 min post treatment with E2. As well, both lines show a modest reduction in $H3K27Me_3$ levels at 4 h (MCF7) or 1 h (T47D) (Figure 5C) indicating a potentially more complex crosstalk mechanism. To further probe the mechanism of this crosstalk, nuclear extracts from MCF7 cells were isolated post E2 stimulation. Consistent with previous studies, PAD2 and ERα co-immunoprecipitate.[17] Notably, PAD2 also co-immunoprecipitates UTX and JMJD3, the two known H3K27 demethylases (Figure 4D). The lack of IP interaction between these demethylases and ERα indicates that the role of ERα is only to recruit PAD2 to the

chromatin. It is then the role of PAD2 to recruit UTX/JMJD3 to facilitate the demethylation of H3K27Me_3.

Crosstalk Regulation of Gene Expression

Using the ER (+) breast cancer model to look directly at gene expression, cells were pretreated with inhibitors or knockdowns of PAD2, EZH2 and UTX/JMJD3 followed by stimulation with E2 and analysis of known ERα-responsive transcripts.[17, 54, 55] By comparing the magnitude of transcriptional stimulation (Figure 6A), the role of each chromatin modifier can be elucidated in the E2-stimulation pathway. Several genes (e.g. GDNF and KRT13) were shown to be downregulated in both the PAD2 KD as well as after treatment with the lysine demethylase inhibitor GSK-J4[56] (Figure 6A). This indicates that PAD2 and the lysine demethylases are both necessary to stimulate transcription in response to E2.

In the cells pretreated with the EZH2 inhibitor EPZ-6438, the basal transcriptional level is increased relative to control cells, even in the absence of estradiol (Figure 6B). These data indicated that reduced methylation of H3K27 facilitates transcription with or without citrullination at key promoters. These results are consistent with a negative crosstalk mechanism resulting in the transcriptional regulation of certain ERα-target genes.

Conclusions

Histone modification crosstalk is a burgeoning facet of epigenetic regulation. While the effect of substrate modifications has a clear impact on enzymatic activity, the multitude of possible histone modifications and modifying enzymes is staggering. Previous studies have cited crosstalk between two or three modifications with gene expression changes. [57–59] In this work, we extend this hypothesis to EZH2-catalyzed H3K27 methylation and PAD2-catalyzed H3R26 citrullination.

Our biochemical studies show a strong negative crosstalk relationship between H3Cit26 and H3K27Me3 wherein citrullination of H3R26 completely blocks methylation on K27 and methylation on H3K27 slows citrullination at R26. To understand why citrullination drastically impacts the methyltransferase activity of EZH2 we modeled peptide substrates with sequences matching histone H3 incorporating either an arginine or citrulline residue at position 26 (Figure 4B). The simplest hypothesis to explain this negative crosstalk would involve the loss of electrostatic interactions between the histone peptide and EZH2 upon the neutralization of the arginine residue. Interestingly, structure based modeling studies show an energetic impact of only a few kcal/mol upon citrullination, not enough to explain the >10,000-fold decrease in k_{cat}/K_M.

Another factor to consider is whether citrullination of the substrate induces a conformational change. Dynamics simulations of the substrate peptides discovered a shift in the ΦΨ angles upon citrullination, where there is a drastic change in structure from β-character to α-character. Such a conformational change would effectively prevent the binding of histone H3 into the active site of EZH2. In support of this analysis, the ΦΨ angles of the H3 peptide modeled into the PRC2 complex (PDB ID 5HYN) agree with those of the wt peptide from

the dynamics analysis (Figure S2). Further supporting our computational findings, CD experiments show a spectral shift consistent with a change in secondary structure upon citrullination of H3R26. In total, our computational and CD measurements are consistent with the citrullination of R26 introducing α-helical character into the region surrounded by this modification (Figure S3).

The effect of methylation on citrullination was less dramatic with a change in catalytic efficiency of 30-fold. This was reflected in the dynamics analysis with only a modest change in the conformation of R26 after trimethylation of the peptide. However, the energetics of the modeling showed a loss of binding energy of around 31 kcal/mol, indicating that the loss of the interaction of the terminal amino group of K27 with different carboxylate residues of PAD2 is the main source of this negative crosstalk interaction.

The negative crosstalk model defined by our biochemical data was recapitulated in cell-based assays in both DLBCL lines as well as an ER (+) breast cancer model. The transcriptional analysis of ERα-target genes under different epigenetic inhibitors and knockdowns provides key insight into the crosstalk regulation of transcription. While it was previously shown that PAD2 is necessary for transcription of several ERα-target genes,[60] this is the first work to suggest that a concurrent K27 demethylation event is also required. By pretreating with the KDM inhibitor GSK-J4, transcription was blocked at many of these promoters similarly to when PAD2 is knocked down. Interestingly, treatment with the EZH2 inhibitor EPZ-6438 increased baseline transcription prior to E2 stimulation. This result could indicate a number of possible epigenetic states: first, the absence of methylation on K27 could allow for faster citrullination of H3R26 (perhaps even without E2 stimulation) and second, that in a K27 unmethylated state, citrullination of R26 is no longer necessary. In this second scenario, the role of PAD2 is entirely to recruit KDMs to the chromatin to demethylate K27 in order to activate transcription.

It should be noted that not all of the gene expression patterns obtained from our qPCR analysis respond in accordance with our model. While all of the genes tested are documented ERα-target genes, they have not all been shown to be PAD2-dependent. If a gene is not PAD2-dependent, that could preclude it from this method of regulation. Secondly, the inhibitors used, particularly the KDM inhibitor GSKJ4, have several off targets that can cause multiple epigenetic effects such as increased lysine methylation elsewhere on histone H3 and H4 which could generate unanticipated or off-target transcriptional changes.

Interestingly, one of the crosstalk-regulated genes is glial derived neurotrophic factor (GDNF). GDNF-Ret signaling has been shown to be a key pathway in ER (+) breast cancers that show resistance to aromatase inhibitors.[17] Combined with our findings that PAD2 and KDM inhibition reduces transcription of GDNF, epigenetic therapy targeting this pathway could be effective against aromatase inhibitor resistant breast cancers.

H3Cit26 is mostly observed in ER (+) breast tumors. Even after E2 stimulation, H3Cit26 signal is lost after 2 h in MCF7 cells and greatly reduced in T47D, indicating a short half-life for the mark. However, basal levels of $H3K27Me_3$ are higher in many cancer cell lines.

In a mass spectrometric analysis of lysine PTMs, LeRoy *et al.* quantified H3K27 methylation states in a wide variety of cell lines. In the majority of cancer cell lines tested, H3K27 was either di- or trimethylated in over 50% of peptides analyzed.[61] The results of our biochemical analysis would indicate that PAD2 is able to citrullinate next to a di- or trimethylated lysine, but at a slower rate. This makes sense as H3K27 spends a majority of time in a highly methylated state. However, EZH2 is strongly inhibited by citrullination in our biochemical model. In the citrullinated state, if UTX or JMJD3 is recruited to demethylate K27, EZH2 will not be able to *re*-methylate K27 until the citrulline mark is removed. It is likely during this state that transcription occurs. A low abundance and short half-life for H3Cit26 diminishes the inhibitory effect on the methyltransferase activity of EZH2 and reduces the active transcription state at these promoters.

In summary, we establish for the first time a negative crosstalk relationship between the citrullination of H3R26 and the methylation of H3K27. This is the first example of citrullination impacting the enzymatic activity of a histone lysine methyltransferase as well as a mutant form of the enzyme that is associated with cancer development. Given the abundance and close proximity of arginine and lysine residues on histones, coupled with the key roles that arginine residues play in substrate recognition for a variety of enzymes, we predict that this type of antagonistic crosstalk is likely to occur elsewhere. More broadly, such antagonistic PTMs may represent a common, yet understudied, mechanism to modulate cell signaling pathways.

METHODS

General

Cell lines (MCF7, T47D, SU-DHL-10, Will-2 and HEK-293T) were purchased from ATCC. Antibodies were purchased from Abcam (H3Cit26 (ab19847)), Cell Signaling (H3 (9715S) and Actin (4967)), Active Motif ($H3K27Me_3$ (39155)), BD (EZH2 (61226)), and Protein Tech (PAD2 (12210-1-AP)). Histone H3, PAD2, PAD4, Rh-PG, BB-F-Amidine and F-Amidine were prepared as previously described.[44, 62–64]

Peptides were synthesized on a PS3 peptide synthesizer (Protein Technologies) with Fmoc-protected amino acids (EMD biosciences) on Rink amide resin (EMD biosciences). Following synthesis, peptides were cleaved from resin and purified by reverse-phase HPLC and correct masses were confirmed by ESI-MS.

Expression and purification of PRC2 complex

The nucleotide sequences encoding full-length human RBBP4 (NP_005601.1) and N-terminal Flag tagged full-length human EZH2 (NP_001190176.1) were inserted into pFastBacDual vector (Invitrogen). The nucleotide sequences encoding full-length human EED (NP_0037 88.2) and N-terminal His-tagged full-length human SUZ12 (NP_056170.2) were inserted into pFastBacDual vector. The nucleotide sequence encoding N-terminal Myc tagged full-length human AEBP2 (NP_694939.2) was inserted into pFastBac1 vector (Invitrogen). Baculovirus generation was carried out according to the protocol of the Bac-to-Bac Baculovirus Expression System (Invitrogen). Sf9 cells were infected at 1.5×10^6

cells/mL using 10 mL each of above three P1 virus per liter of culture and incubated at 28 °C for 48 h. Cells were harvested and stored at −80 °C for subsequent protein purification. Protein purification was conducted at 4 °C. Frozen cell pellets from 2 L cultures were lysed by incubation with stirring in 100 mL of lysis buffer (50 mM Tris-HCl pH 7.5, 300 mM NaCl, 10% glycerol, 0.1% Triton X-100, Roche complete protease inhibitor cocktail, 5 U/mL Benzonase) and homogenization. Cell lysates were clarified by centrifugation in a Beckman JA-18 rotor for 30 min at 16,500 rpm. The supernatant was incubated with 5 mL of anti-Flag M2 resin (Sigma) for 3 h. The resin was then packed onto a column and washed with buffer A (buffer (50 mM Tris-HCl pH 7.5, 300 mM NaCl, and 10% glycerol) and buffer B (buffer (50 mM Tris-HCl pH 7.5, 150 mM NaCl, and 10% glycerol). The protein was eluted with buffer B containing 0.1 mg/mL of Flag peptide (Sigma). Fractions containing EZH2 complex were pooled and the protein concentration was determined by the Bradford assay using BSA as a standard. The protein was aliquotted and stored at −80 °C. The EZH2 (Y641N) complex was generated the same way as wild-type EZH2 complex except the above EZH2 wild-type sequences were replaced by EZH2 (Y641N) sequences using PCR-based mutagenesis.

PAD pretreatment of PRC2 complex or Histone H3 followed by PAD inhibition

PAD2 or PAD4 (10 nM) was incubated with the PRC2 complex (0.1 mg/mL) for 60 min in PAD reaction buffer (100 mM Tris pH 7.6, 10 mM $CaCl_2$, 2 mM DTT, and 50 mM NaCl) before adding 1 mM of F-Amidine. Inhibition was allowed to proceed for 15 min before adding Histone H3 (3 μM), S-[methyl-^{14}C]-adenosyl methionine (SAM) (Perkin Elmer NEC363010UC) to a final concentration of 15 μM, and altering the buffer composition to PRC2 conditions (50 mM Tris pH 8.5, 10 mM DTT). The PRC2 methyltransferase reaction was allowed to proceed for 120 min before quenching with 6× SDS-PAGE loading dye and the samples were processed for analysis as described previously.[46]

The reverse preincubation reaction was also performed wherein PAD2 or PAD4 was preincubated with Histone H3 and the PRC2 complex and [methyl-^{14}C] SAM was added. Briefly, PAD2 or PAD4 was incubated with Histone H3 (30 μM) for 60 min in PAD reaction buffer before adding F-Amidine (1 mM) to inhibit PAD activity. Inhibition was allowed to proceed for 15 min before adding PRC2 complex (0.01 mg/mL), [methyl-^{14}C] SAM (Perkin Elmer NEC363010UC) (15 μM final) and altering the buffer composition to PRC2 conditions (50 mM Tris pH 8.5 and 10 mM DTT). The PRC2 methyltransferase reaction was allowed to proceed for 120 min before quenching with 6× SDS-PAGE loading dye and analysis as described previously.[65] Note that under these conditions, F-Amidine completely inhibits the PAD reaction, but has no effect on the methyltransferase activity of PRC2.

PAD Activity post PRC2 Incubation with H3 Substrates

Histone H3 or peptide substrates were incubated with PRC2 (13 μg/mL) in PRC2 reaction buffer (50 mM Tris pH 8.5, 10 mM DTT) and 15 μM of SAM (Sigma A7007) for 120 min before adding either PAD2 or PAD4 (100 nM) and PAD reaction buffer (100 mM Tris pH 7.6, 10 mM $CaCl_2$, 2 mM DTT, 50 mM NaCl). The citrullination reaction was incubated at 37 °C for 30 min before quenching with 100% TCA to a final concentration of 20%. Citrullination levels were determined using the citrulline-specific probe Rh-PG using

methods described previously.[65] Briefly, Rh-PG (1 mM final) was added to the acid-quenched samples and allowed to incubate for 30 min at 37 °C. After this period, the probe was quenched with 500 mM citrulline in 50 mM HEPES pH 7.6 (to a final concentration of 100 mM citrulline) for 30 min at 37 °C. The reactions were then placed on ice for 30 min to allow for protein precipitation followed by centrifugation at 16,000 × g for 15 min at 4 °C. The supernatants were removed and the pellet was washed with ice cold acetone and centrifuged again at 16,000 × g for 15 min at 4 °C. The supernatants were again discarded and the recovered pellets were allowed to air dry for 5 min at 100 °C to remove acetone. The pellets were resuspended in 100 mM arginine in 50 mM HEPES pH 7.6 before separating the reaction components by SDS-PAGE. Fluorescent bands were imaged on a Typhoon scanner (λ_{ex} = 532 nm, λ_{em} = 580 nm). Gel bands were quantified using ImageQuant.

PAD Activity Assay

PAD2 or PAD4 (100 nM) was incubated in PAD reaction buffer (100 mM Tris pH 7.6, 10 mM $CaCl_2$, 2 mM DTT, 50 mM NaCl) with 1 mM Histone H3 peptide substrate for 30 min before quenching in liquid nitrogen. Samples were analyzed for citrulline content using the COLDER assay as previously described.[44]

PRC2 Activity Assay

PRC2 complex (0.66 μg/mL) in 50 mM Tris pH 8.5 plus 10 mM DTT with 15 μM [methyl-^{14}C] SAM (Perkin Elmer NEC363010UC) and Histone H3 (3 μM) was incubated for 120 min at 25 °C before quenching with 6× SDS-PAGE loading dye and analysis by PAGE as described previously.[66]

Kinetic Analysis

Initial rates were analyzed using GraphPad Prism 6 software. Kinetic constants were determined using the following equation:

$$v = V_{max}[S]/(K_M + [S]), \quad (1)$$

Generation of PAD2 and EZH2 Knockdown Cell lines

Mission shRNA constructs were purchased from Sigma (PAD2 TRCN0000051447, EZH2 TRCN0000286227) and transfected into HEK 293T cells (FuGene HD) with lentiviral packaging mix (Sigma SHP001) according to the manufacturer's protocols. Lentiviral particles were collected in the media 48 h post transfection and used to infect SU-DHL-10 and Will-2 cells according to the Mission protocol for lentiviral infection of suspension cell lines. After 3 days of lentiviral incubation, 1 μg/mL of puromycin (Corning 61385RA) was used to select for infected cells to generate stable cell lines. SU-DHL-10 and Will-2 knockdown cells were assayed 7–10 days after stable knockdown. For MCF7 and T47D cells, stable lines were not viable and cells were assayed 5 days post lentiviral infection.

Analysis of H3K27Me$_3$ Levels from Cell Lysate

Cells were lysed in 0.4 M HCl on ice for 30 min before centrifugation. Protein concentration was determined using the BioRad DC assay (BioRad 5000111). Acid extracted lysates were neutralized using Balance buffer (Epigentek OP-0006-100) diluted in buffer (MSD R60TX-3) to a final concentration of 8 μg/mL and kept on ice. Meanwhile, a custom MULTI-SPOT® 96-well 4-spot Histone H3 plate was blocked with 150 μL 3% BSA in wash buffer (MSD R61TX-1) for 1 h at room temperature on a plate shaker. The plate was washed three times with 300 μL wash buffer before adding 25 μL of cell lysate to the appropriate wells. Lysate was incubated on the plate overnight at 4 °C on a plate shaker. The following day, the plate was washed three times with 300 μL wash buffer followed by the addition of custom detection antibody (SULFO-TAG® Histone H3 K27Me$_3$ antibody) for 2 h at room temperature on a plate shaker. The antibody solution was then removed and replaced immediately with 100 μL 2% formaldehyde (Mallinckrodt 5016-02) in PBS (Gibco 14190-136) and incubated for 30 min at room temperature on a plate shaker. The plate was washed three times with wash buffer and 150 μL Read Buffer (MSD R92TC-3) was added immediately before reading on a SECTOR imager.

Estradiol Stimulation of MCF7 Cells

MCF7 and T47D cells were maintained in phenol red-free MEM (Gibco 17-305-CV) with L-Glutamine (2 mM, Gibco 25030), non-essential amino acids (Gibco 11140-050) and 10% charcoal-stripped FBS (Corning 35072CV). Cells were treated with either 100 nM β-estradiol (Sigma Aldrich E2758) or ethanol for times ranging from 30 min to 6 h. Cells were washed with ice-cold PBS and harvested by scraping into ice-cold PBS. Cells were lysed by acid extraction in 0.4 M HCl for the detection of histones by Western blotting.

Co-Immunoprecipitation of PAD2 and ERα

MCF7 cells were stimulated with estradiol as above followed by nuclear extract isolation using a Nuclear Extract Co-IP kit (Active Motif 54001). 1 mg of lysate from each sample was rocked overnight at 4 °C with either 1 μg PAD2, 1 μg ERα, or no antibody. The following day, IP samples were added to a protein G agarose column (Active Motif 53039) and rocked for 2 h at 4 °C. Washes were performed as indicated in the manufacturer's protocol prior to elution with reducing buffer (130 mM Tris pH 6.8, 4% SDS, 0.02% Bromophenol Blue, 100 mM DTT) at 37 °C for 15 min. An equal volume of glycerol was added to the eluted samples prior to Western analysis.

qPCR Analysis

MCF7 or T47D cells (wt or PAD2 KD) were treated for 5 days total with 5 μM EPZ-6438 (Cayman Chemical 10403254-99-8) or 400 nM GSK-J4 (Sigma SML0701) with the final two days in phenol red-free MEM (Gibco 17-305-CV) with L-Glutamine (2 mM, Gibco 25030), non-essential amino acids (Gibco 11140-050) and 10% charcoal-stripped FBS (Corning 35072CV). Estradiol stimulation was conducted as described above. RNA was isolated from the cells using RNeasy Mini Kit (Qiagen 47104) and treated with DNase I (Invitrogen 18068-015) according to the manufacturer's protocol. Reverse transcription was performed using Superscript III First-Strand (Invitrogen 18080-051) followed by treatment

with RNase (included in kit). qPCR primers were purchased from ThermoFisher TaqMan Gene Expression Analysis. Primer catalog numbers can be found in Table S1. qPCR was carried out using Maxima Probe/ROX qPCR Mastermix (Thermo K0233) and cDNA titrated in a linear range on a Applied Biosystems ViiA 7 Real Time PCR System.

Computational methods

We used molecular modeling tools to calculate interaction energies between H3 substrates and their receptors before and after post translational modification of R26Cit and K273Met. The interaction energies were calculated by Molecular Operating Environment (MOE) 2013.08 (Chemical Computing Group Inc., Montreal, QC, Canada). To analyze the impact of K27 trimethylation on the binding energy to the PRC2 complex we used the X-ray structure of a human PRC2 bound to the H3K27M peptide.[65] To investigate the impact of R26 citrullination, we used the X-ray structures of PAD2[67] and PAD4 in complex with o-F-amidine,[68] a peptide based inhibitor that mimics an arginine residue bound to the enzyme. For these studies, we superimposed the PAD2 structure (PDB ID: 4N2C) on to PAD4 (PDB ID: 3B1U) and then transferred the peptidomimentic inhibitor from PAD4 to PAD2. To assess H3 sequence propensity to adopt receptor binding conformation in solutions we ran dynamic simulations for 10 ns on each 3D representation of H3 WT and modified. For dynamics simulations we used Discovery Studio (DS) (Dassault Systèmes). Each of the simulations was started from the same conformation of H3 peptide. For both MOE and DS, we used the CHARMm force field for energy calculations and dynamics simulations.

Supplementary Material

Refer to Web version on PubMed Central for supplementary material.

Acknowledgments

This work was supported in part by NIH grants GM079357, GM110394, and GM118112 to P.R.T. K.W.C. was supported by the Lilly Innovation Fellowship Award (LIFA) program sponsored by Eli Lilly.

ABBREVIATIONS

BB-F-Amidine	*N*1-[1,4′-Phenyl]benzoyl-*N*5-(2-fluoro-1-inimoethyl)-1-(1H-benzo[d]imidazole-2-yl)-L-ornithine amide
E2	17-β-estradiol
EED	Embryonic Ectoderm Development
ERα	Estrogen receptor α
ER (+)	Estrogen receptor positive
EZH2	Enhancer of Zeste Homolog 2
F-Amidine	*N*-α-benzoyl-*N*5-(2-fluoro-1-iminoethyl)-L-ornithine amide
h	Hour(s)

HCl	Hydrochloric Acid
H3	Histone H3
Rh-PG	*N*-(((3-Glyoxal)phenylamino)propionyl)-1*H*-1,2,3-triazol-4-yl)methyl-5(6)-carboxamidotetramethyl rhodamine hydrate
min	minute(s)
PAD2	Protein Arginine Deiminase type-2
PAD4	Protein Arginine Deiminase type-4
PRC2	Polycomb Repressive Complex 2
PTM	Posttranslational Modification
SAM	S-Adenosyl Methionine
Suz12	Suppressor of Zeste Homolog 12
Wt	wild-type

References

1. Grunstein M. Histone acetylation in chromatin structure and transcription. Nature. 1997; 389:349–352. [PubMed: 9311776]
2. Workman JL, Kingston RE. Alteration of nucleosome structure as a mechanism of transcriptional regulation. Annu Rev Biochem. 1998; 67:545–579. [PubMed: 9759497]
3. Venkatesh S, Workman JL. Histone exchange, chromatin structure and the regulation of transcription. Nat Rev Mol Cell Biol. 2015; 16:178–189. [PubMed: 25650798]
4. Kadoch C, Crabtree GR. Mammalian SWI/SNF chromatin remodeling complexes and cancer: Mechanistic insights gained from human genomics. Sci Adv. 2015; 1:e1500447. [PubMed: 26601204]
5. Pfister NT, Fomin V, Regunath K, Zhou JY, Zhou W, Silwal-Pandit L, Freed-Pastor WA, Laptenko O, Neo SP, Bargonetti J, Hoque M, Tian B, Gunaratne J, Engebraaten O, Manley JL, Borresen-Dale AL, Neilsen PM, Prives C. Mutant p53 cooperates with the SWI/SNF chromatin remodeling complex to regulate VEGFR2 in breast cancer cells. Genes Dev. 2015; 29:1298–1315. [PubMed: 26080815]
6. Baylin SB. DNA methylation and gene silencing in cancer. Nat Clin Pract Oncol. 2005; 2(Suppl 1):S4–11. [PubMed: 16341240]
7. Lee JS, Shilatifard A. A site to remember: H3K36 methylation a mark for histone deacetylation. Mutat Res. 2007; 618:130–134. [PubMed: 17346757]
8. Walter W, Clynes D, Tang Y, Marmorstein R, Mellor J, Berger SL. 14-3-3 interaction with histone H3 involves a dual modification pattern of phosphoacetylation. Mol Cell Biol. 2008; 28:2840–2849. [PubMed: 18268010]
9. Weake VM, Workman JL. Histone ubiquitination: triggering gene activity. Mol Cell. 2008; 29:653–663. [PubMed: 18374642]
10. Hsu JM, Chen CT, Chou CK, Kuo HP, Li LY, Lin CY, Lee HJ, Wang YN, Liu M, Liao HW, Shi B, Lai CC, Bedford MT, Tsai CH, Hung MC. Crosstalk between Arg 1175 methylation and Tyr 1173 phosphorylation negatively modulates EGFR-mediated ERK activation. Nat Cell Biol. 2011; 13:174–181. [PubMed: 21258366]

11. Yamagata K, Daitoku H, Takahashi Y, Namiki K, Hisatake K, Kako K, Mukai H, Kasuya Y, Fukamizu A. Arginine methylation of FOXO transcription factors inhibits their phosphorylation by Akt. Mol Cell. 2008; 32:221–231. [PubMed: 18951090]
12.
13. Vossenaar ER, Zendman AJ, van Venrooij WJ, Pruijn GJ. PAD, a growing family of citrullinating enzymes: genes, features and involvement in disease. Bioessays. 2003; 25:1106–1118. [PubMed: 14579251]
14. Fuhrmann J, Clancy KW, Thompson PR. Chemical biology of protein arginine modifications in epigenetic regulation. Chem Rev. 2015; 115:5413–5461. [PubMed: 25970731]
15. Christophorou MA, Castelo-Branco G, Halley-Stott RP, Oliveira CS, Loos R, Radzisheuskaya A, Mowen KA, Bertone P, Silva JC, Zernicka-Goetz M, Nielsen ML, Gurdon JB, Kouzarides T. Citrullination regulates pluripotency and histone H1 binding to chromatin. Nature. 2014; 507:104–108. [PubMed: 24463520]
16. Hagiwara T, Hidaka Y, Yamada M. Deimination of histone H2A and H4 at arginine 3 in HL-60 granulocytes. Biochemistry. 2005; 44:5827–5834. [PubMed: 15823041]
17. Zhang X, Bolt M, Guertin MJ, Chen W, Zhang S, Cherrington BD, Slade DJ, Dreyton CJ, Subramanian V, Bicker KL, Thompson PR, Mancini MA, Lis JT, Coonrod SA. Peptidylarginine deiminase 2-catalyzed histone H3 arginine 26 citrullination facilitates estrogen receptor alpha target gene activation. Proc Natl Acad Sci U S A. 2012; 109:13331–13336. [PubMed: 22853951]
18. Cuthbert GL, Daujat S, Snowden AW, Erdjument-Bromage H, Hagiwara T, Yamada M, Schneider R, Gregory PD, Tempst P, Bannister AJ, Kouzarides T. Histone deimination antagonizes arginine methylation. Cell. 2004; 118:545–553. [PubMed: 15339660]
19. Wang Y, Wysocka J, Sayegh J, Lee YH, Perlin JR, Leonelli L, Sonbuchner LS, McDonald CH, Cook RG, Dou Y, Roeder RG, Clarke S, Stallcup MR, Allis CD, Coonrod SA. Human PAD4 regulates histone arginine methylation levels via demethylimination. Science. 2004; 306:279–283. [PubMed: 15345777]
20. De Rycke L, Nicholas AP, Cantaert T, Kruithof E, Echols JD, Vandekerckhove B, Veys EM, De Keyser F, Baeten D. Synovial intracellular citrullinated proteins colocalizing with peptidyl arginine deiminase as pathophysiologically relevant antigenic determinants of rheumatoid arthritis-specific humoral autoimmunity. Arthritis Rheum. 2005; 52:2323–2330. [PubMed: 16052592]
21. Lundberg K, Nijenhuis S, Vossenaar ER, Palmblad K, van Venrooij WJ, Klareskog L, Zendman AJ, Harris HE. Citrullinated proteins have increased immunogenicity and arthritogenicity and their presence in arthritic joints correlates with disease severity. Arthritis Res Ther. 2005; 7:R458–467. [PubMed: 15899032]
22. Musse AA, Li Z, Ackerley CA, Bienzle D, Lei H, Poma R, Harauz G, Moscarello MA, Mastronardi FG. Peptidylarginine deiminase 2 (PAD2) overexpression in transgenic mice leads to myelin loss in the central nervous system. Dis Model Mech. 2008; 1:229–240. [PubMed: 19093029]
23. McElwee JL, Mohanan S, Griffith OL, Breuer HC, Anguish LJ, Cherrington BD, Palmer AM, Howe LR, Subramanian V, Causey CP, Thompson PR, Gray JW, Coonrod SA. Identification of PADI2 as a potential breast cancer biomarker and therapeutic target. BMC Cancer. 2012; 12:500. [PubMed: 23110523]
24. Cherrington BD, Morency E, Struble AM, Coonrod SA, Wakshlag JJ. Potential role for peptidylarginine deiminase 2 (PAD2) in citrullination of canine mammary epithelial cell histones. PLoS One. 2010; 5:e11768. [PubMed: 20668670]
25. Cherrington BD, Zhang X, McElwee JL, Morency E, Anguish LJ, Coonrod SA. Potential role for PAD2 in gene regulation in breast cancer cells. PLoS One. 2012; 7:e41242. [PubMed: 22911765]
26. Mohanan S, Cherrington BD, Horibata S, McElwee JL, Thompson PR, Coonrod SA. Potential role of peptidylarginine deiminase enzymes and protein citrullination in cancer pathogenesis. Biochem Res Int. 2012; 2012:895343. [PubMed: 23019525]
27. Guertin MJ, Zhang X, Anguish L, Kim S, Varticovski L, Lis JT, Hager GL, Coonrod SA. Targeted H3R26 deimination specifically facilitates estrogen receptor binding by modifying nucleosome structure. PLoS Genet. 2014; 10:e1004613. [PubMed: 25211228]

28. Kanduri M, Sander B, Ntoufa S, Papakonstantinou N, Sutton LA, Stamatopoulos K, Kanduri C, Rosenquist R. A key role for EZH2 in epigenetic silencing of HOX genes in mantle cell lymphoma. Epigenetics. 2013; 8:1280–1288. [PubMed: 24107828]
29. McCabe MT, Ott HM, Ganji G, Korenchuk S, Thompson C, Van Aller GS, Liu Y, Graves AP, Della Pietra A, Diaz E 3rd, LaFrance LV, Mellinger M, Duquenne C, Tian X, Kruger RG, McHugh CF, Brandt M, Miller WH, Dhanak D, Verma SK, Tummino PJ, Creasy CL. EZH2 inhibition as a therapeutic strategy for lymphoma with EZH2-activating mutations. Nature. 2012; 492:108–112. [PubMed: 23051747]
30. Knutson SK, Kawano S, Minoshima Y, Warholic NM, Huang KC, Xiao Y, Kadowaki T, Uesugi M, Kuznetsov G, Kumar N, Wigle TJ, Klaus CR, Allain CJ, Raimondi A, Waters NJ, Smith JJ, Porter-Scott M, Chesworth R, Moyer MP, Copeland RA, Richon VM, Uenaka T, Pollock RM, Kuntz KW, Yokoi A, Keilhack H. Selective inhibition of EZH2 by EPZ-6438 leads to potent antitumor activity in EZH2-mutant non-Hodgkin lymphoma. Mol Cancer Ther. 2014; 13:842–854. [PubMed: 24563539]
31. Lee SR, Roh YG, Kim SK, Lee JS, Seol SY, Lee HH, Kim WT, Kim WJ, Heo J, Cha HJ, Kang TH, Chung JW, Chu IS, Leem SH. Activation of EZH2 and SUZ12 Regulated by E2F1 Predicts the Disease Progression and Aggressive Characteristics of Bladder Cancer. Clin Cancer Res. 2015; 21:5391–5403. [PubMed: 26268246]
32. Katona BW, Liu Y, Ma A, Jin J, Hua X. EZH2 inhibition enhances the efficacy of an EGFR inhibitor in suppressing colon cancer cells. Cancer Biol Ther. 2014; 15:1677–1687. [PubMed: 25535899]
33. Yin Y, Qiu S, Peng Y. Functional roles of enhancer of zeste homolog 2 in gliomas. Gene. 2016; 576:189–194. [PubMed: 26435191]
34. Fu Y, Chen J, Pang B, Li C, Zhao J, Shen K. EZH2-induced H3K27me3 is associated with epigenetic repression of the ARHI tumor-suppressor gene in ovarian cancer. Cell Biochem Biophys. 2015; 71:105–112. [PubMed: 25077680]
35. McCabe MT, Graves AP, Ganji G, Diaz E, Halsey WS, Jiang Y, Smitheman KN, Ott HM, Pappalardi MB, Allen KE, Chen SB, Della Pietra A, Dul E 3rd, Hughes AM, Gilbert SA, Thrall SH, Tummino PJ, Kruger RG, Brandt M, Schwartz B, Creasy CL. Mutation of A677 in histone methyltransferase EZH2 in human B-cell lymphoma promotes hypertrimethylation of histone H3 on lysine 27 (H3K27). Proc Natl Acad Sci U S A. 2012; 109:2989–2994. [PubMed: 22323599]
36. Guglielmelli P, Biamonte F, Score J, Hidalgo-Curtis C, Cervantes F, Maffioli M, Fanelli T, Ernst T, Winkelman N, Jones AV, Zoi K, Reiter A, Duncombe A, Villani L, Bosi A, Barosi G, Cross NC, Vannucchi AM. EZH2 mutational status predicts poor survival in myelofibrosis. Blood. 2011; 118:5227–5234. [PubMed: 21921040]
37. Konze KD, Ma A, Li F, Barsyte-Lovejoy D, Parton T, Macnevin CJ, Liu F, Gao C, Huang XP, Kuznetsova E, Rougie M, Jiang A, Pattenden SG, Norris JL, James LI, Roth BL, Brown PJ, Frye SV, Arrowsmith CH, Hahn KM, Wang GG, Vedadi M, Jin J. An orally bioavailable chemical probe of the Lysine Methyltransferases EZH2 and EZH1. ACS Chem Biol. 2013; 8:1324–1334. [PubMed: 23614352]
38. Verma SK, Tian X, LaFrance LV, Duquenne C, Suarez DP, Newlander KA, Romeril SP, Burgess JL, Grant SW, Brackley JA, Graves AP, Scherzer DA, Shu A, Thompson C, Ott HM, Aller GS, Machutta CA, Diaz E, Jiang Y, Johnson NW, Knight SD, Kruger RG, McCabe MT, Dhanak D, Tummino PJ, Creasy CL, Miller WH. Identification of Potent, Selective, Cell-Active Inhibitors of the Histone Lysine Methyltransferase EZH2. ACS Med Chem Lett. 2012; 3:1091–1096. [PubMed: 24900432]
39. Montgomery ND, Yee D, Chen A, Kalantry S, Chamberlain SJ, Otte AP, Magnuson T. The murine polycomb group protein Eed is required for global histone H3 lysine-27 methylation. Curr Biol. 2005; 15:942–947. [PubMed: 15916951]
40. Pasini D, Bracken AP, Jensen MR, Lazzerini Denchi E, Helin K. Suz12 is essential for mouse development and for EZH2 histone methyltransferase activity. EMBO J. 2004; 23:4061–4071. [PubMed: 15385962]
41. Kim W, Bird GH, Neff T, Guo G, Kerenyi MA, Walensky LD, Orkin SH. Targeted disruption of the EZH2-EED complex inhibits EZH2-dependent cancer. Nat Chem Biol. 2013; 9:643–650. [PubMed: 23974116]

42. Arrowsmith CH, Bountra C, Fish PV, Lee K, Schapira M. Epigenetic protein families: a new frontier for drug discovery. Nat Rev Drug Discov. 2012; 11:384–400. [PubMed: 22498752]
43. Su IH, Basavaraj A, Krutchinsky AN, Hobert O, Ullrich A, Chait BT, Tarakhovsky A. Ezh2 controls B cell development through histone H3 methylation and Igh rearrangement. Nat Immunol. 2003; 4:124–131. [PubMed: 12496962]
44. Bicker KL, Subramanian V, Chumanevich AA, Hofseth LJ, Thompson PR. Seeing citrulline: development of a phenylglyoxal-based probe to visualize protein citrullination. J Am Chem Soc. 2012; 134:17015–17018. [PubMed: 23030787]
45. Luo Y, Arita K, Bhatia M, Knuckley B, Lee YH, Stallcup MR, Sato M, Thompson PR. Inhibitors and inactivators of protein arginine deiminase 4: functional and structural characterization. Biochemistry. 2006; 45:11727–11736. [PubMed: 17002273]
46. Luo Y, Knuckley B, Lee YH, Stallcup MR, Thompson PR. A fluoroacetamidine-based inactivator of protein arginine deiminase 4: design, synthesis, and in vitro and in vivo evaluation. J Am Chem Soc. 2006; 128:1092–1093. [PubMed: 16433522]
47. Bradley WD, Arora S, Busby J, Balasubramanian S, Gehling VS, Nasveschuk CG, Vaswani RG, Yuan CC, Hatton C, Zhao F, Williamson KE, Iyer P, Mendez J, Campbell R, Cantone N, Garapaty-Rao S, Audia JE, Cook AS, Dakin LA, Albrecht BK, Harmange JC, Daniels DL, Cummings RT, Bryant BM, Normant E, Trojer P. EZH2 inhibitor efficacy in non-Hodgkin's lymphoma does not require suppression of H3K27 monomethylation. Chem Biol. 2014; 21:1463–1475. [PubMed: 25457180]
48. Xie H, Xu J, Hsu JH, Nguyen M, Fujiwara Y, Peng C, Orkin SH. Polycomb repressive complex 2 regulates normal hematopoietic stem cell function in a developmental-stage-specific manner. Cell Stem Cell. 2014; 14:68–80. [PubMed: 24239285]
49. Bohers E, Mareschal S, Bouzelfen A, Marchand V, Ruminy P, Maingonnat C, Menard AL, Etancelin P, Bertrand P, Dubois S, Alcantara M, Bastard C, Tilly H, Jardin F. Targetable activating mutations are very frequent in GCB and ABC diffuse large B-cell lymphoma. Genes Chromosomes Cancer. 2014; 53:144–153. [PubMed: 24327543]
50. Chen C, Zhao M, Yin N, He B, Wang B, Yuan Y, Yu F, Hu J, Yin B, Lu Q. Abnormal histone acetylation and methylation levels in esophageal squamous cell carcinomas. Cancer Invest. 2011; 29:548–556. [PubMed: 21843048]
51. Rogenhofer S, Kahl P, Mertens C, Hauser S, Hartmann W, Buttner R, Muller SC, von Ruecker A, Ellinger J. Global histone H3 lysine 27 (H3K27) methylation levels and their prognostic relevance in renal cell carcinoma. BJU Int. 2012; 109:459–465. [PubMed: 21810159]
52. Wigle TJ, Knutson SK, Jin L, Kuntz KW, Pollock RM, Richon VM, Copeland RA, Scott MP. The Y641C mutation of EZH2 alters substrate specificity for histone H3 lysine 27 methylation states. FEBS Lett. 2011; 585:3011–3014. [PubMed: 21856302]
53. Yap DB, Chu J, Berg T, Schapira M, Cheng SW, Moradian A, Morin RD, Mungall AJ, Meissner B, Boyle M, Marquez VE, Marra MA, Gascoyne RD, Humphries RK, Arrowsmith CH, Morin GB, Aparicio SA. Somatic mutations at EZH2 Y641 act dominantly through a mechanism of selectively altered PRC2 catalytic activity, to increase H3K27 trimethylation. Blood. 2011; 117:2451–2459. [PubMed: 21190999]
54. Charpentier AH, Bednarek AK, Daniel RL, Hawkins KA, Laflin KJ, Gaddis S, MacLeod MC, Aldaz CM. Effects of estrogen on global gene expression: identification of novel targets of estrogen action. Cancer Res. 2000; 60:5977–5983. [PubMed: 11085516]
55. Jin VX, Leu YW, Liyanarachchi S, Sun H, Fan M, Nephew KP, Huang TH, Davuluri RV. Identifying estrogen receptor alpha target genes using integrated computational genomics and chromatin immunoprecipitation microarray. Nucleic Acids Res. 2004; 32:6627–6635. [PubMed: 15608294]
56. Lin CY, Strom A, Vega VB, Kong SL, Yeo AL, Thomsen JS, Chan WC, Doray B, Bangarusamy DK, Ramasamy A, Vergara LA, Tang S, Chong A, Bajic VB, Miller LD, Gustafsson JA, Liu ET. Discovery of estrogen receptor alpha target genes and response elements in breast tumor cells. Genome Biol. 2004; 5:R66. [PubMed: 15345050]
57. Kruidenier L, Chung CW, Cheng Z, Liddle J, Che K, Joberty G, Bantscheff M, Bountra C, Bridges A, Diallo H, Eberhard D, Hutchinson S, Jones E, Katso R, Leveridge M, Mander PK, Mosley J, Ramirez-Molina C, Rowland P, Schofield CJ, Sheppard RJ, Smith JE, Swales C, Tanner R,

Thomas P, Tumber A, Drewes G, Oppermann U, Patel DJ, Lee K, Wilson DM. A selective jumonji H3K27 demethylase inhibitor modulates the proinflammatory macrophage response. Nature. 2012; 488:404–408. [PubMed: 22842901]

58. Zippo A, Serafini R, Rocchigiani M, Pennacchini S, Krepelova A, Oliviero S. Histone crosstalk between H3S10ph and H4K16ac generates a histone code that mediates transcription elongation. Cell. 2009; 138:1122–1136. [PubMed: 19766566]
59. Warnock LJ, Adamson R, Lynch CJ, Milner J. Crosstalk between site-specific modifications on p53 and histone H3. Oncogene. 2008; 27:1639–1644. [PubMed: 17891183]
60. Lan J, Lepikhov K, Giehr P, Walter J. Histone and DNA methylation control by H3 serine 10/threonine 11 phosphorylation in the mouse zygote. Epigenetics Chromatin. 2017; 10:5. [PubMed: 28228845]
61. Morandi A, Martin LA, Gao Q, Pancholi S, Mackay A, Robertson D, Zvelebil M, Dowsett M, Plaza-Menacho I, Isacke CM. GDNF-RET signaling in ER-positive breast cancers is a key determinant of response and resistance to aromatase inhibitors. Cancer Res. 2013; 73:3783–3795. [PubMed: 23650283]
62. Leroy G, Dimaggio PA, Chan EY, Zee BM, Blanco MA, Bryant B, Flaniken IZ, Liu S, Kang Y, Trojer P, Garcia BA. A quantitative atlas of histone modification signatures from human cancer cells. Epigenetics Chromatin. 2013; 6:20. [PubMed: 23826629]
63. Thompson PR, Kurooka H, Nakatani Y, Cole PA. Transcriptional coactivator protein p300. Kinetic characterization of its histone acetyltransferase activity. J Biol Chem. 2001; 276:33721–33729. [PubMed: 11445580]
64. Knight JS, Subramanian V, O'Dell AA, Yalavarthi S, Zhao W, Smith CK, Hodgin JB, Thompson PR, Kaplan MJ. Peptidylarginine deiminase inhibition disrupts NET formation and protects against kidney, skin and vascular disease in lupus-prone MRL/lpr mice. Ann Rheum Dis. 2015; 74:2199–2206. [PubMed: 25104775]
65. Osborne TC, Obianyo O, Zhang X, Cheng X, Thompson PR. Protein arginine methyltransferase 1: positively charged residues in substrate peptides distal to the site of methylation are important for substrate binding and catalysis. Biochemistry. 2007; 46:13370–13381. [PubMed: 17960915]
66. Knipp M, Vasak M. A colorimetric 96-well microtiter plate assay for the determination of enzymatically formed citrulline. Anal Biochem. 2000; 286:257–264. [PubMed: 11067748]
67. Justin N, Zhang Y, Tarricone C, Martin SR, Chen S, Underwood E, De Marco V, Haire LF, Walker PA, Reinberg D, Wilson JR, Gamblin SJ. Structural basis of oncogenic histone H3K27M inhibition of human polycomb repressive complex 2. Nat Commun. 2016; 7:11316. [PubMed: 27121947]
68. Slade DJ, Fang P, Dreyton CJ, Zhang Y, Fuhrmann J, Rempel D, Bax BD, Coonrod SA, Lewis HD, Guo M, Gross ML, Thompson PR. Protein arginine deiminase 2 binds calcium in an ordered fashion: implications for inhibitor design. ACS Chem Biol. 2015; 10:1043–1053. [PubMed: 25621824]

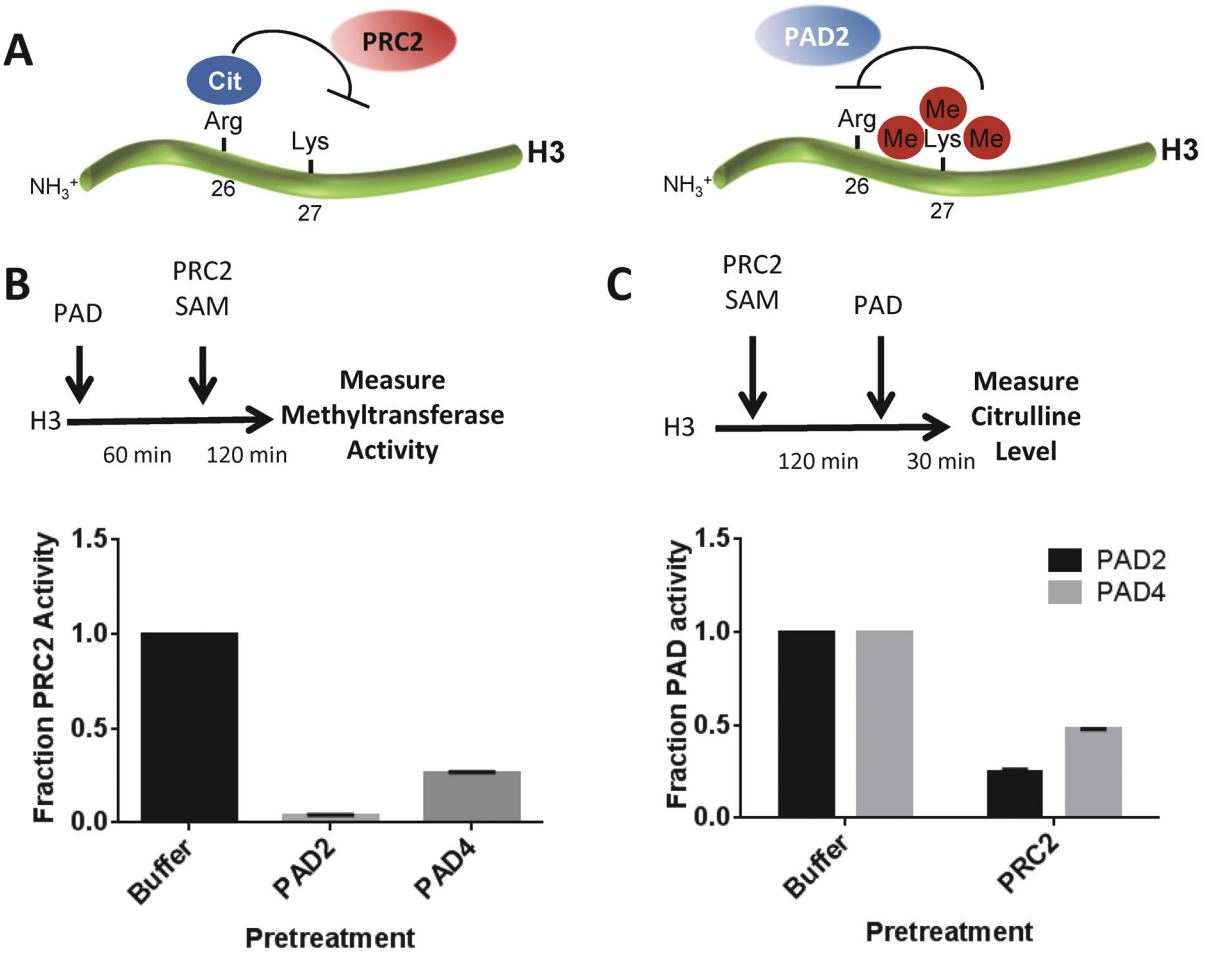

Figure 1.

Crosstalk between the citrullination activity of PADs 2 and 4 and the methyltransferase activity of the PRC2 complex on Histone H3. (A) Schematic representation of proposed crosstalk between H3R26Cit and H3K27Me$_3$. (B) Recombinant histone H3 was citrullinated by 100 nM PAD2 or PAD4 for 1 h prior to the addition of 50 nM of the PRC2 complex with 15 μM SAM for 2 h. PRC2 activity was measured in a ^{14}C radiolabeled PAGE assay. (C) Recombinant histone H3 was methylated by 50 nM of the PRC2 complex with 15 μM SAM for 2 h before the addition of 100 nM PAD2 or PAD4 for 30 minutes. Citrulline levels were measured using the citrulline-specific chemical probe (Rh-PG).

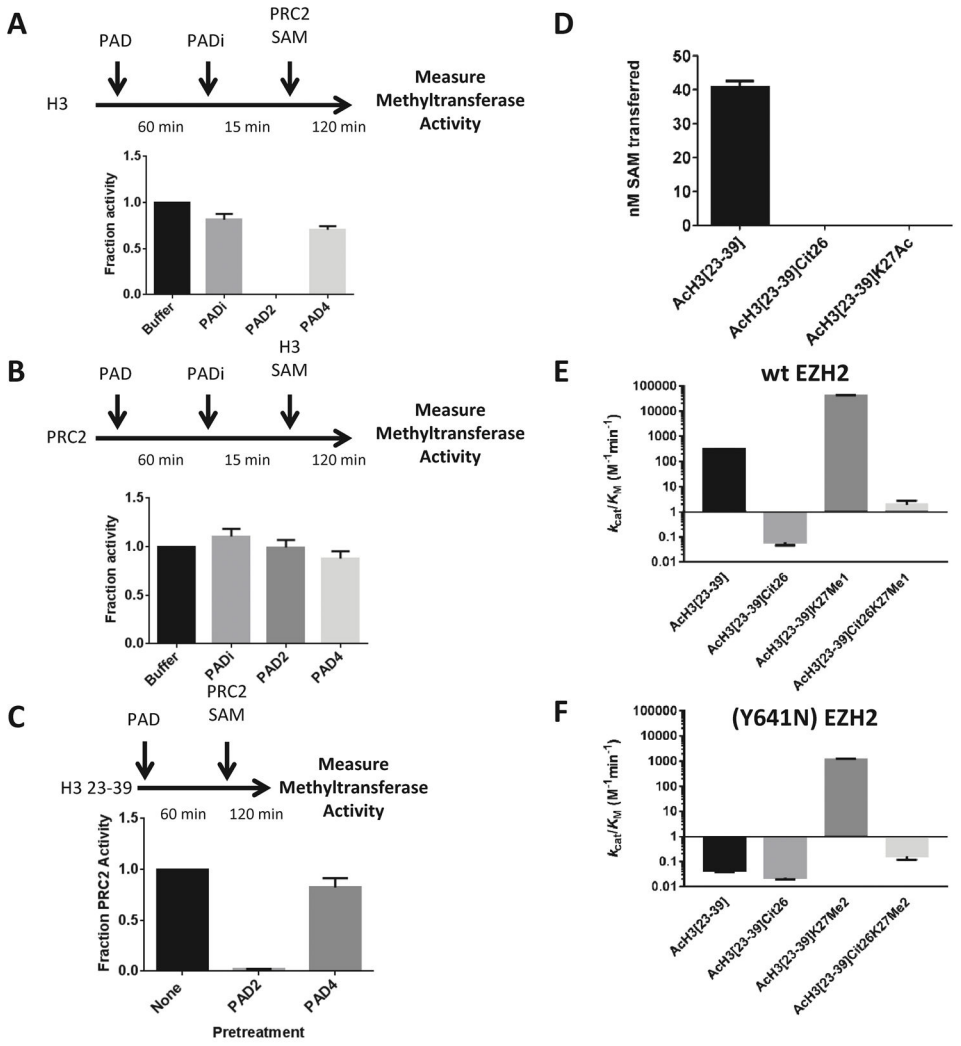

Figure 2.

PADs 2 and 4 inhibit PRC2-mediated methylation of histone H3 by modifying the histone. (A) PAD2 and PAD4 (10 nM) were preincubated with histone H3, followed by the addition of the PAD-specific inhibitor F-Amidine (1 mM). The residual methyltransferase activity was then measured using a gel-based radioactivity assay. Activity was normalized to the buffer control and is displayed as a fraction of this control. (B) PAD2 and PAD4 (10 nM) were preincubated with the PRC2 complex, followed by PAD inhibition with F-Amidine (1 mM). The measurement of residual methyltransferase activity shows that citrullination of the PRC2 complex does not impair its methyltransferase activity. (C) PAD2 and PAD4 were preincubated with a histone H3 tail analog encompassing both R26 and K27. This peptide was used because it only contains one arginine residue (R26). Thus, any effects on PRC2 activity can be attributed to the modification of R26 only. (D) A synthetic peptide containing citrulline in the place of R26 is not methylated by PRC2 complex. As a control, we show that a K27Ac containing peptide is also not methylated by the PRC2 complex. Both the Cit26 peptide as well as the K27Ac peptide showed no detectable product formation. (E,F) Methyltransferase activity of the PRC2 complex containing wt (E) or EZH2 (Y641N) (F)

was measured with the indicated peptide substrate. k_{cat}/K_M is plotted to show the reduction in activity upon citrulline incorporation into the peptide substrates in the place of R26. The steady-state kinetic parameters are provided in Tables S2 and S3.

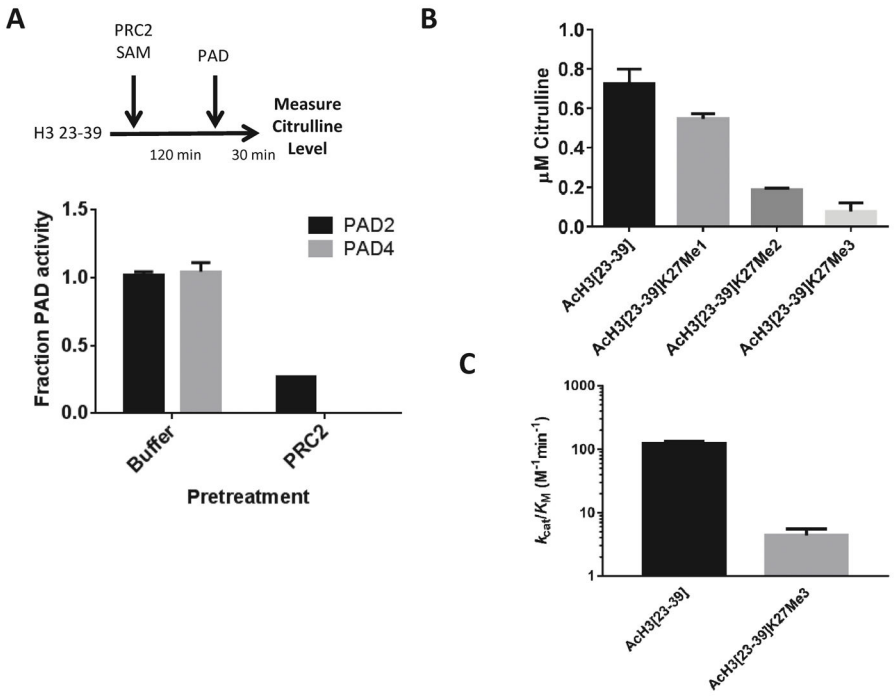

Figure 3.

Citrullination of H3R26 is reduced by the methylation of H3 peptide substrates at K27. (A) The $H3^{23–39}$ peptide was preincubated with the PRC2 complex or a buffer control before assaying PAD2 or PAD4 deimination activity. Citrulline levels were determined with Rh-PG. (B) $H3^{23–39}$ peptides were synthesized with various K27 methylation states. The effect of these modifications on PAD2 activity was evaluated using the COLDER assay. (C) PAD2-catalyzed deimination activity (k_{cat}/K_M) with different peptides displays the reduction in activity upon trimethylation of K27. The steady-state kinetic parameters are provided in Table S4.

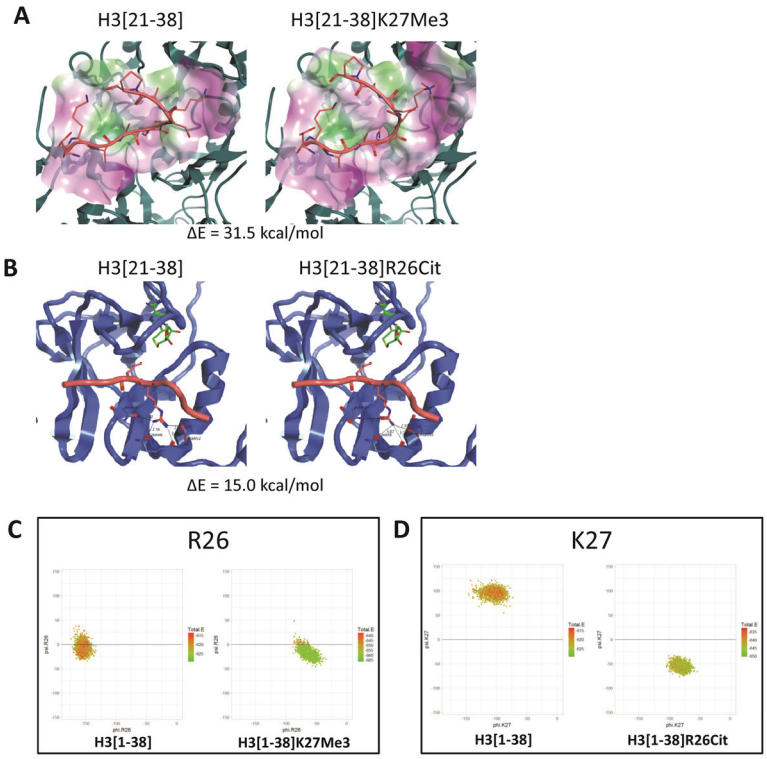

Figure 4.

Structural Rationale for PTM Crosstalk. (A) H3[22–30] peptides were modeled into PAD4 (PDB ID: 3B1U) with the PAD2 structure (PDB ID: 4N2C) overlaid. Wt sequence and K27Me3 together show no steric hinderance in binding upon methylation of K27. (B) H3[22–30] peptides were modeled into the PRC2 complex (PDB ID: 5HYN). Wt sequence show hydrogen bonding interactions between the peptide R26 and three EZH2 residues. R26Cit peptide shows a disruption of some interactions, causing a change in binding energy of 15 kcal/mol. (C,D) Peptide Dynamics Studies Show Conformational Change upon Citrullination. Ramachandran plots of H3R26 (C) and H3K27 (D) after dynamics analysis of histone H3 peptides [1–38]. (C) The conformation of R26 is only slightly altered between the wt sequence and K27Me3 indicating only a slight change in orientation of R26 after K27 has been trimethylated by PRC2. (D) The conformation of K27 changes drastically from β-character in the wt sequence to α-character when position 26 is citrulline.

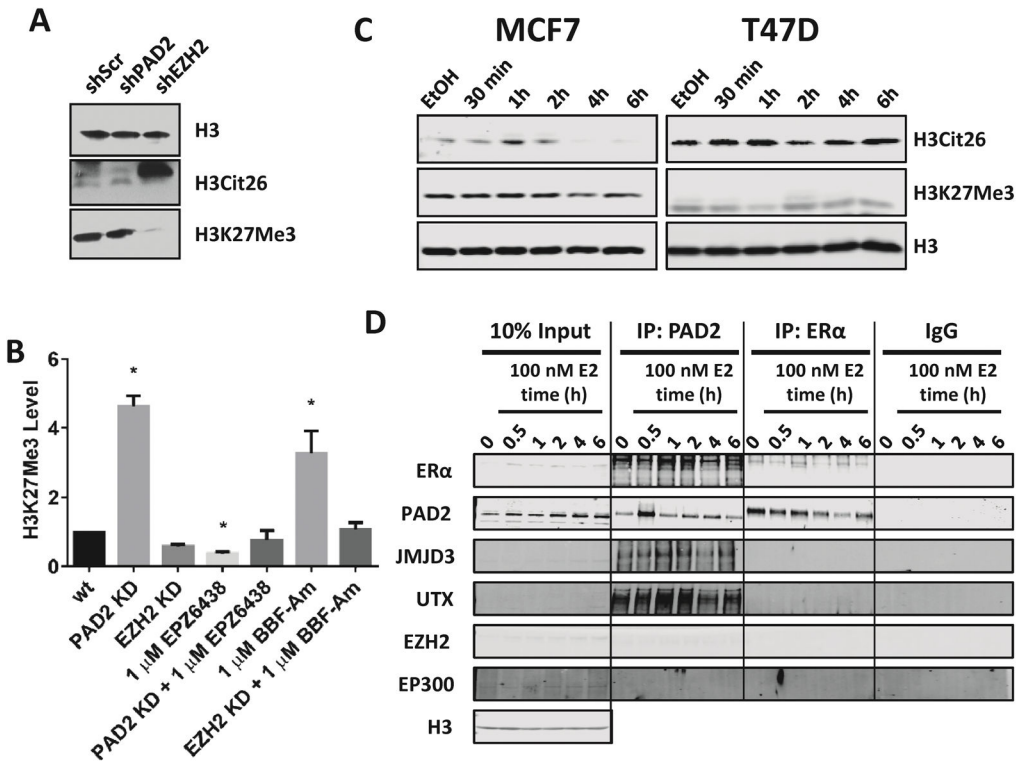

Figure 5.

Cellular models of crosstalk between H3R26Cit and H3K27Me3. (A) SU-DHL-10 cells show changes in global H3 PTMs upon knockdown of PAD2 and EZH2. (B) Will-2 cells show changes in global H3K27Me3 levels upon knockdown of PAD2 and EZH2 as well as upon treatment with the PAD inhibitor BB-F-Amidine. * $p < 0.05$ (C) ER(+) Breast cancer lines were stimulated with 100 nM 17-β-estradiol post 48 h hormone starvation in phenol red-free media. Formation of H3Cit26 is observed over time as well as a modest reduction in H3K27Me3 levels at 4 h (MCF7) and 1 h (T47D). (D) Nuclear extracts from MCF7 cells treated as above with 17-β-estradiol were immunoprecipiated with antibodies for PAD2 and ERα to probe for interacting proteins. Two lysine demethylases for H3K27, JMJD3 and UTX, were pulled down with PAD2.

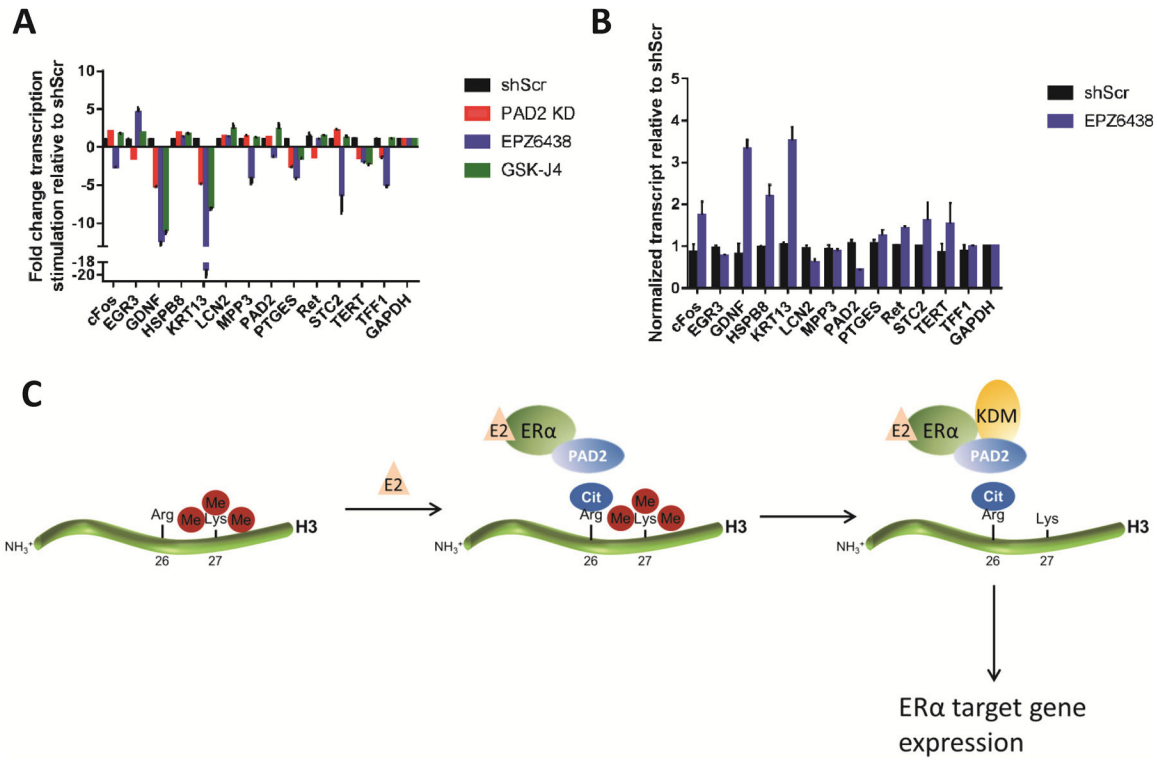

Figure 6.

Histone PTM Crosstalk Regulation of Gene Expression in ER(+) Breast Cancer Lines. (A,B) T47D cells were pretreated for 5 days with 5 μM EPZ-6438 or 400 nM GSK-J4, PAD2 lentivirus or control with the final two days in hormone starvation medium. Cells were then stimulated with estradiol and harvested at key timepoints. (A) Baseline and peak of transcription (60 min) were compared to obtain the fold change in transcription stimulation. (B) Baseline transcription levels of EPZ-6438 treated cells compared to control cells show increases in transcription prior to estradiol stimuation. (C) Model of PTM crosstalk transcriptional regulation. Upon E2 stimulation, ERα recruits PAD2 to the chromatin to citrullinate H3R26. PAD2 recruits a KDM (either UTX or JMJD3) to demethylate K27, which activates transcription or ERα target genes.